

An alpine lacustrine record of early Holocene North American Monsoon dynamics from Dry Lake, southern California (USA)

Broxton W. Bird* and Matthew E. Kirby

Department of Geological Sciences, California State University, Fullerton, Fullerton, California 92834 USA;

**Author for correspondence (broxton.bird@gmail.com)*

Received 21 February 2005; accepted in revised form 31 May 2005

Key words: Climate change, Dry Lake, Early Holocene, North American Monsoon, Southern California

Abstract

Dry Lake (2763 m), located in the San Bernardino Mountains of southern California, USA, provides a high-resolution climate record from the coastal southwest depicting early Holocene terrestrial climate. 27 AMS ^{14}C dates and multi-proxy analyses, including magnetic susceptibility, total organic matter, microfossil counts, and grain size, suggest the early Holocene was significantly wetter than present, due to an enhanced North American Monsoon (NAM). Elevated insolation at 9000 cal year B.P., raised summer sea surface temperatures in the Gulf of California and the eastern tropical Pacific, as well as land surface temperatures, extending the NAM into southern California. The data also provide evidence of the 8.2 ka event, which registers as a 300-year cool period characterized by reduced monsoonal precipitation, depressed basin productivity, and increased erosion. We suggest this event is the most likely period for the early to middle Holocene (9000–5000 cal year B.P.) glacial advance in the San Bernardino Mountains proposed by Owen et al. (2003, *Geology* 31: 729–732).

Introduction

The nature of early Holocene (defined for this paper as the period from 9000 to 7500 cal year B.P.) terrestrial climate change in the coastal southwest is not well characterized. This problem arises mainly from the fact that long-term (> 5000-years), regional records of terrestrial climate are scarce. Furthermore, the resolution of the scarce early Holocene records are limited to millennial-scale climate interpretations (e.g., Enzel et al. 1992; Kirby et al. 2005). These records, however, indicate that the coastal southwest was significantly wetter during the early Holocene in response to varied seasonal insolation. Notably, these findings are in agreement with the results from recent climate modeling studies, which suggest that the early Holocene summer insolation

maximum strengthened the North American Monsoon (NAM), resulting in greater effective moisture in the southwestern United States (Webber 2001; Liu et al. 2003). While these studies are insightful, important questions still remain concerning higher-frequency early Holocene climate variability in the coastal southwestern United States.

In order to address these questions, we present a well-dated, high-resolution lacustrine record of early Holocene climate from Dry Lake in the San Bernardino Mountains of southern California, USA (Figure 1). This study is part of a larger research initiative to understand terrestrial Holocene climate in the coastal southwest using the rare, but natural, lakes of southern California. In this paper we focus on the interval from 9000 and 6500 cal year B.P. in order to explore two main issues: (1)

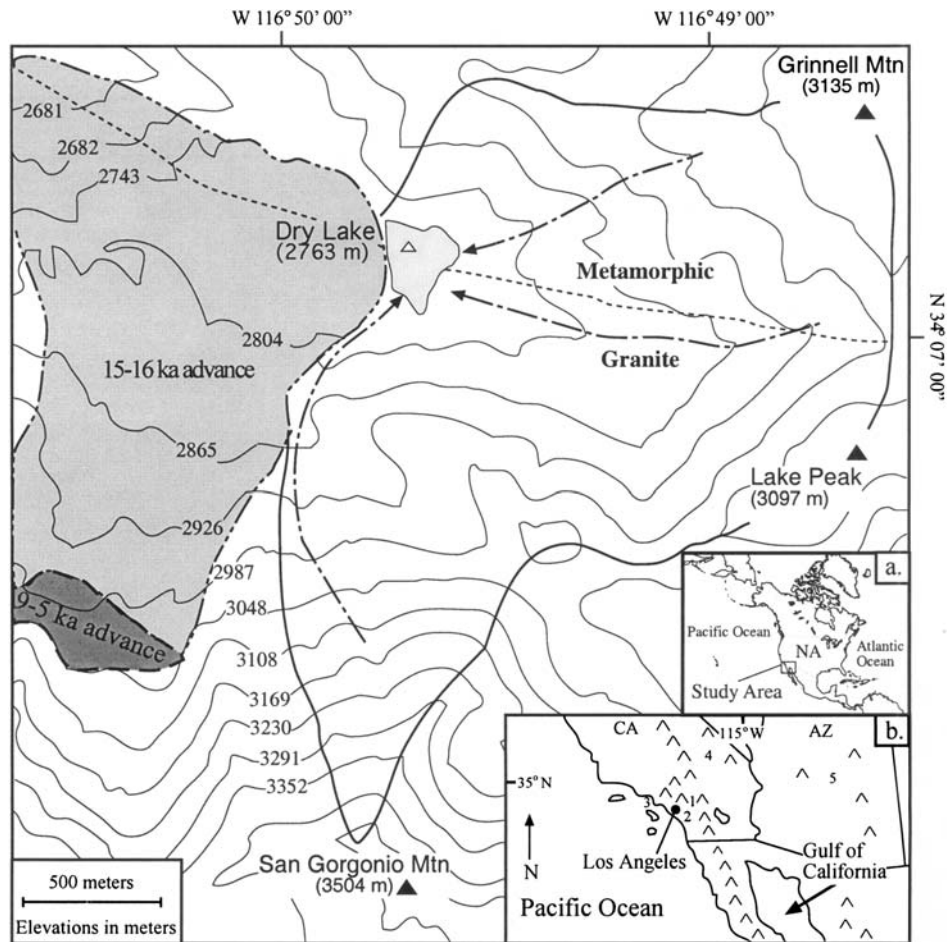


Figure 1. Topographic map of the Dry Lake basin with inset maps (a and b) showing the global and regional location of Dry Lake (1). Other sites depicted on the coastal southwestern regional map (b) are Lake Elsinore (2), the Santa Barbara Basin (3), Silver Lake (4), and Montezuma Well (5). Identified on the topographic map are the core location (represented by an open triangle), the 15–16 and 9–5 ka glacial advances proposed by Owen et al. (2003) (double dashed lines), the drainage basin area (solid line), ephemeral streams (dashed arrows) and lithology (modified from Morton et al. 1980). (Modified from USGS San Gorgonio and Moonridge 1:24,000 7.5' quadrangles).

What is the influence of the early Holocene summer insolation maximum on regional climate in the coastal southwest with a specific focus on the NAM; and, (2) what is the evidence, if any, for the 8200-year 'cool' event (hereafter referred to as the 8.2 ka event; Alley et al. 1997).

Regional climatology

The coastal southwestern United States is characterized by a Mediterranean climate with a winter precipitation maximum and summer minimum (Figure 2; Cayan and Roads 1984). Winter

precipitation is controlled chiefly by southerly displacement of the polar front jet stream, which redirects cold fronts, extratropical cyclones, and associated troughs from the northern Pacific into the study region (Weaver 1962; Pyke 1972; Hirschboeck 1985). Exceptionally wet winters are often associated with the occurrence of El Niño/Southern Oscillation (ENSO) (Ropelewski and Halpert 1986; Schonher and Nicholson 1989; Redmond and Kotch 1991; Ely et al. 1994; Cayan et al. 1999). During an El Niño event, a strong southerly branch of the jet stream develops over southern California, directing moisture from the north Pacific and eastern tropical Pacific into the

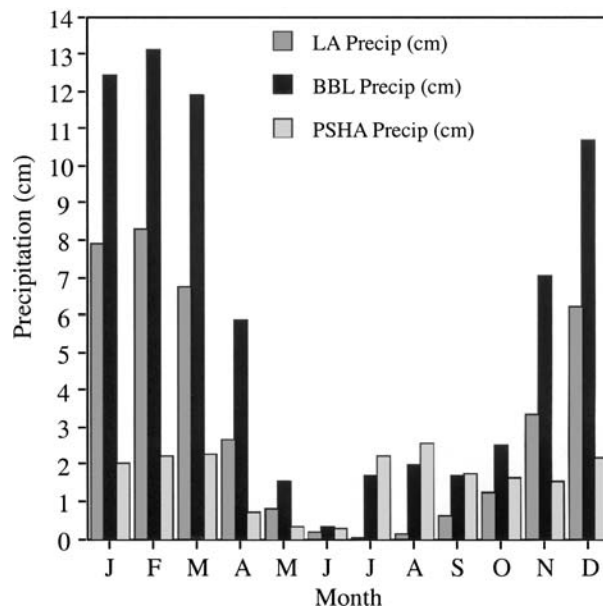


Figure 2. Average monthly precipitation at Big Bear Lake (BBL; 1933–2002), Los Angeles (L.A.; 1878–2002), and Phoenix Sky Harbor Airport (PSHA; 1948–2002) from National Climate Data Center weather observation stations (<http://www.ncdc.noaa.gov/oa/climate/stationlocator.html>). Note the July–August–September precipitation peak at BBL. This peak is mainly caused by the North American Monsoon and local convection and, to a lesser degree, Pacific-derived tropical cyclones.

region, producing severe precipitation events lasting one to several days (Mo and Higgins 1998).

Summers (June–July–August) are typically dry, as strengthened sub-tropical high-pressure over the southwest and eastern Pacific displaces the polar front jet stream to a more northerly latitude (Figure 2; Trewartha 1981). Occasionally, the coastal southwest receives anomalous summer precipitation associated with either tropical cyclones or convective storms. The most extreme events are associated with large rouge tropical cyclones or ‘chuboscas’ emanating from the eastern tropical Pacific (Hereford et al. 2004). Normally, tropical cyclones follow a northwesterly storm track away from land, where they weaken and decay upon reaching cooler waters of the northern Pacific (Webb and Betancourt 1992). Sometimes, however, cyclones recurve eastward and landfall along the coastal southwest, causing significant precipitation (Webb and Betancourt 1992; Hereford et al. 2004). Other, typically less dramatic sources of summer precipitation are convective storms, either isolated or associated with an expanded NAM (Tubbs 1972). The contribution of summer precipitation to annual totals is strongly dependent on topography, and is best

defined in the mountain regions surrounding the Los Angeles Basin, such as Big Bear Lake in the San Bernardino Mountains (Figure 2).

While the coastal southwest is characterized by maximum winter precipitation, the desert southwest experiences peak precipitation during the summer (Figure 2; Webb and Betancourt 1992). Like the southwestern coastal regions, winter precipitation is the result of a southerly displaced jet stream and associated frontal systems and troughs (Pyke 1972; Webb and Betancourt 1992). Summer precipitation, however, is primarily derived from the NAM, a meteorological phenomenon typically restricted to Arizona, New Mexico, and northern Mexico (Webb and Betancourt 1992; Adams and Comrie 1997). Recent studies have demonstrated that the modern NAM is fundamentally linked to increased summer insolation through a series of ocean/atmosphere interactions. One of the most significant components of the NAM is the northward migration of elevated sea surface temperatures (SSTs; $>26^{\circ}\text{C}$) in the Gulf of California (GOC), which are generated by enhanced summer insolation (Mitchell et al. 2002). From May to June, warm waters incrementally migrate to the northern GOC via surface currents

and tidal mixing, sparking the NAM monsoon within three days of arriving (Mitchell et al. 2002). Of note, severe monsoon seasons are typically initiated when SSTs in the GOC exceed 29 °C. Moisture surges (also gulf surges), another important component of the NAM, are also influenced by summer insolation (Hales Jr. 1972; Brenner 1974; Higgins et al. 2004). Moisture surges are derived from the passage of easterly tropical waves and associated disturbances (i.e., cyclones) past the southern mouth of the GOC. With enhanced summer insolation, deep convection and easterly tropical waves become more frequent, resulting in greater moisture delivery up the GOC and into the NAM region (Higgins et al. 2004). In addition, summer insolation helps to establish strong upper level anticyclonic circulation over the central United States and thermal low pressure in the desert southwest. These circulation patterns aid the advection of moisture from the eastern tropical Pacific up the GOC and into the southwestern United States (Higgins et al. 2004).

Study area

Dry Lake (2763 m) is a moraine dammed alpine 'playa' lake located at the headwaters of the Santa Ana River in the San Geronio Wilderness of southern California (Figure 1). The Dry Lake drainage basin is small, about 3.7 km², and underlain by biotite gneiss and schist basement to the north and quartz monzonite basement to the south (Morton et al. 1980; Figure 1). Vegetation surrounding the Dry Lake basin is largely coniferous forest, mainly comprised of *Pinus contorta* and *P. flexilis* with a sparse shrub understory of *Castanopsis sempervirens* and *Arctostaphylos patula* var. *stachyphylla* (Minnich 1984).

Because instrumental precipitation data is lacking from Dry Lake, we use monthly total precipitation data collected from Big Bear Lake and Big Bear Dam between 1933 and 2002 to characterize the San Bernardino Mountains, and thus Dry Lake. Characteristic of the coastal southwest, Dry Lake experiences a Mediterranean climate with peak precipitation occurring between November and April (Figure 2). Due to the seasonality of storms, precipitation falls mainly as snow at and above 2750 m, averaging 70–100 cm year⁻¹ water equivalent (Minnich 1986).

Strong southwesterly winds during winter storms strip snow from windward slopes and redistribute it on northeasterly leeward slopes causing disproportionate accumulation on these aspects (Minnich 1984). Such transport is significant enough that one third of exceptionally heavy snow years result in perennial snow on San Geronio Mountain (Minnich 1984). Summer precipitation is only 7.5% of the annual average total at Dry Lake, but the peak during July–August reflects the limited contribution of the NAM, local convective storms, and occasional land falling cyclones (Figure 2). While there are no detailed lake level data for Dry Lake, and although currently dry, Dry Lake has been observed to hold water year round after extreme wet winters, such as the exceptionally wet year of 1992 (<http://www.sgwa.org/gallery.htm>).

Methods

Core collection

Using an Eijkelkamp hand-coring device, two cores, comprised of 27 (30×4 cm²) segments totaling 8.4 m (DLPC03-1 and DLPC03-2), were extracted from the depositional center of Dry Lake (Figure 1). The depositional center was determined using a hand-held global positioning system unit to identify the lowest point in the currently dry lakebed. In addition, the strike and dip of the bedrock and glacial features, which create the basin, were extrapolated to define an approximate basin geometry, from which, we identified the depositional center. After extraction, the cores were transported to the Paleoclimate Laboratory at California State University, Fullerton (CSUF), USA, where they were split, described and sub-sampled for sediment analyses. Sub-sampling for the initial analyses of magnetic susceptibility (CHI), and loss on ignition (LOI) was performed at 1 cm intervals, while grain size and microfossil counts were measured at 5, and 10 cm intervals with 1 cm resolution over transitions and depositional features of interest. The sub-sampling process consumed one half of the split core. The second half was archived and stored at the cold storage facility at the CSUF Paleoclimate Laboratory. Despite excellent overall recovery, some gaps exist in the sediment record. We attribute these gaps to the coring process, but because of the excellent age

control, these gaps are accounted for and assumed to be real gaps in sediment and time.

Age control and age model

Age control was established by AMS ^{14}C dating of 27 charcoal samples taken from cores DLPC03-1 and DLPC03-2 at the University of California, Irvine's Keck Carbon Cycle AMS Facility (Table 1 and Figure 3). Radiocarbon dates were converted to calendar years before present (cal year B.P.) using the web-based program Calib 4.0 (Stuiver and Reimer 1993). All ages referred to hereafter are calibrated unless otherwise noted. An age-model was constructed using 20 of the 27 AMS ^{14}C dates. Seven dates were eliminated because they were collected from rapidly deposited layers (RDLs, i.e., storm events; term from St-Onge et al. 2004). RDLs were identified by visual observation of disrupted sediment as well as from inconsistent CHI, %TOM, and grain-size (i.e., %sand) trends. The remaining 20 dates were plotted versus depth, assuming linear sedimentation between points. To account for RDLs in the age model, the basal contact was assigned the age generated from initial linear regressions between AMS ^{14}C dates. The top contact age was assigned the basal contact age plus one year to model an instantaneous event. Subsequent equations generated from linear regressions between dates were used to convert depths to ages, against which all data were plotted (Figure 3).

Sedimentology

The analyses used in this study were chosen in order to characterize the various components of the Dry Lake depositional system, including productivity, system energy, and terrestrial input (i.e., weathering). Percent total organic matter (%TOM) and total carbonate (%TC) were determined by weighing the initial sediment sample and then combusting each sub-sample at 550 and 950 °C, respectively, for 2 h. After combustion, the samples were reweighed and the residual weight was subtracted from the original weight to determine the percent weight loss (Dean 1974; Heiri et al. 2001; Boyle 2004). %TC is not discussed further, as all values were 3% or below,

precluding useful interpretation (Dean 1974; Heiri et al. 2001). Mass magnetic susceptibility (CHI; $\times 10^{-7} \text{ m}^3 \text{ kg}^{-1}$) was immediately measured after sub-sampling on all samples using the using a Barington MS2 magnetic susceptibility meter. The final CHI was calculated by dividing the average of two measurements (rotated y -axis per measurement) by the wet sediment weight to account for differences in mass (Thompson et al. 1975; e.g., Lanci et al. 1999). Microfossil counts of charcoal were performed at 5–10 cm intervals (1 cm intervals were used over transitions and RDLs) using a binocular microscope. Samples were prepared by wet sieving at 125 μm , after which they were dried and weighed. Counts of split samples were multiplied by the number of splits and a correction factor, determined by dividing the dry sediment weight by 5, to normalize all results as counts per 5 g of dry sediment (e.g., MacDonald et al. 1991). Percent sand (74.00–2000 μm), silt (3.9–73.99 μm), and clay (0.02–3.89 μm) were measured at 5 cm intervals (1 cm intervals over transitions and RDLs) using the Malvern Mastersizer 2000 laser diffraction particle analyzer (e.g., Warner and Domack 2002). Sediment samples measuring 1 cm^3 were pre-treated with 10–40 ml of a 30% H_2O_2 solution at 100 °C for 2 h in order to remove the organic fraction prior to particle analysis. Sample measurements were performed using a refractive index of 1.52 with water as the dispersant. Five measurement cycles per sample were averaged to for the final grain size percentages.

Analysis of historical summer precipitation

Precipitation data from the Big Bear Lake, CA, (hereafter referred to as Big Bear) and Phoenix Sky Harbor Airport, AZ, (hereafter referred to as Phoenix) National Climate Data Center weather observation stations were analyzed in order to explore relationships between summer precipitation (July–August) in the San Bernardino Mountains and the desert southwest during the NAM. The NCEP-NCAR reanalysis database (Kalnay et al. 1995) was then used to construct plots of surface precipitable water over the southwestern United States and GOC. From these plots we are able to characterize the spatial relationships of atmospheric conditions during

Table 1. Radiocarbon dates.

Identification	Core depth (cm)	Conventional radiocarbon Age ^a	2-Sigma calibrated age ^b (cal year B.P.)	2-Sigma average calibrated age (cal year B.P.)
UCI-2573 ^c	8.5	320 ± 30	307–462	380
UCI-2574 ^c	12.5	805 ± 45	660–792	726
UCI-6826 ^c	17.5	1470 ± 25	1308–1407	1357
UCI-2576 ^c	45.5	1635 ± 25	1420–1471	1450
UCI-2577 ^c	88.5	2750 ± 25	2778–1471	2830
UCI-2578 ^c	106.5	3635 ± 25	3865–3990	3930
UCI-2579 ^c	167.5	3980 ± 30	4303–4308	4310
UCI-2580 ^c	205.5	4455 ± 25	4968–5074	5020
UCI-2581 ^c	260.5	5390 ± 25	6001–6011	6010
UCI-2582 ^c	267.5	5605 ± 40	6299–6450	6380
UCI-2583 ^c	283.5	5825 ± 25	6504–6505	6510
UCI-2584	297.5	6365 ± 45	7210–7221	7220
UCI-2585 ^c	317.5	6185 ± 35	6951–6960	6960
UCI-2586 ^c	399.5	6890 ± 25	7666–7756	7710
UCI-2587 ^c	484.5	7080 ± 25	7793–7797	7800
UCI-2588 ^c	508.5	7240 ± 50	7959–8166	8060
UCI-2589 ^c	609.5	7355 ± 30	8033–8090	8150
UCI-2590	645.5	7895 ± 25	8579–8777	8690
UCI-2591	679.5	7835 ± 25	8540–8649	8600
UCI-2592 ^c	716.5	7740 ± 30	8426–8561	8490
UCI-2593	750.5	7675 ± 25	8393–8461	8427
UCI-2594	745.5	8020 ± 50	8653–8668	8660
UCI-2595	759.5	7820 ± 50	8430–8439	8440
UCI-2597 ^c	807.5	7990 ± 25	8721–8735	8730
UCI-6827	822.5	8060 ± 25	8979–9029	9000
UCI-6828 ^c	840.5	7970 ± 25	8745–8996	8870
Beta-188743 ^c	841.5	8090 ± 40	8990–9095	9040

^aStuiver and Polach (1977).

^bStuiver and Reimer (1993).

^cDates used in age model.

summers with severe precipitation intervals common to both Phoenix and Big Bear so as to determine the degree to which the present-day NAM influences precipitation in the San Bernardino Mountains.

Results

Sedimentology

Except for the top 10 cm, which appears to be a poorly developed soil horizon, the cores are comprised of lacustrine sediments derived from the surrounding basin. Silt is the main sediment constituent throughout the cores. Interbedded with the silt are sand layers (1–10 cm thick), some of which are capped by organic deposits of wood, charcoal, and plant material and bounded on the bottom by erosional surfaces. Sand content is

highly variable from 9000 to 8100 (Figure 4b). Maximum values are reached in two distinct peaks at 8230 and 8100, after which, there is a first-order decreasing trend to 6500 with a single peak at 7700 (Figure 4b). CHI is relatively low from 9000 to 8400, at which point variability increases (Figure 4c). Values peak at 8230 and 8100 and then generally decrease again with some scattered peaks from 8100 to 6500 (Figure 4c). %TOM is most variable from 9000 to 8400, characterized by high values (Figure 4d). After 8400, %TOM declines but still displays some variability until 7300 (Figure 4d). After 7300 there is only a single peak at 6700 (Figure 4d). Charcoal is high and variable from 9000 to 7600, but it is interrupted by a 300-year period from 8400 to 8100 of significantly reduced counts. After 7600, charcoal is only a minor sediment constituent, although it is still present in measurable quantities throughout the core.

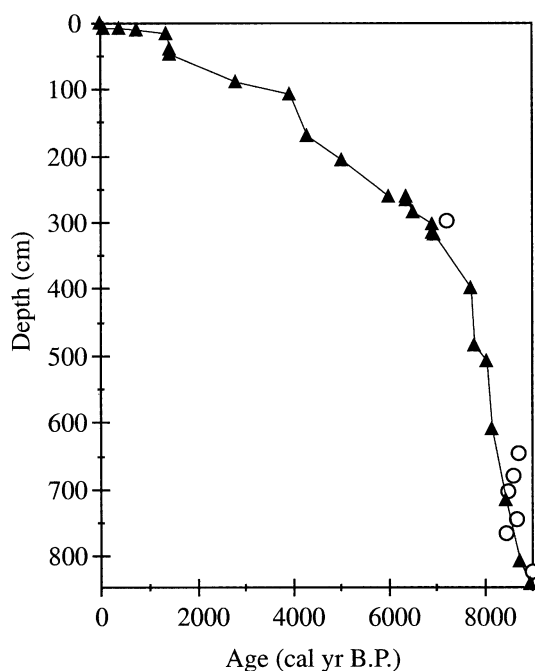


Figure 3. Age model of combined cores DLPC03-1 and DLPC03-2. Dates used in the age model are represented by triangles; removed dates are shown with open circles.

Analysis of historical summer precipitation

Summer monsoon precipitation (July–August) at Phoenix is well correlated ($r = 0.58$, $\alpha > 0.001$) with July–August precipitation at Big Bear (Figure 5). Plots of the two datasets demonstrate contemporaneous extreme wet summers (rainfall $> 1SD$) in 1951, 1955 and 1984 (Figure 5). Plots of anomalous July–August precipitable surface water constructed for these years illustrates a strong regional positive anomaly over southern California and southwestern Arizona during the events (Figure 6).

Discussion

Proxy interpretation

For this paper, %TOM is interpreted in two ways: (1) intervals of sustained, high %TOM represent an overall increase in productivity (i.e., greater local biomass) during periods of greater wetness; and, (2) spikes in %TOM represent severe precipitation events, when the influx of

organic detritus is instantly increased to the lake from the surrounding basin. Similar to %TOM, charcoal counts are interpreted as an indicator of basin productivity as well as storm events. Generally elevated charcoal is interpreted to reflect greater terrestrial biomass in response to increased effective moisture, which then provides increased fuel for forest fires. Spikes in charcoal are interpreted to reflect sudden influxes of charcoal fragments in response to abrupt increases in runoff (i.e., storm events). Grain size is interpreted to indicate the relative energy of the depositional environment. Therefore, elevated sand content and sand spikes are interpreted as storm events or periods of increased storminess. CHI is interpreted to reflect the contribution of terrestrial material (i.e., weathered bedrock) eroded into the lake system from the surrounding drainage basin (Thompson et al. 1975; Lanci et al. 1999). In order to preserve CHI in the sediment record, the magnetic minerals (i.e., magnetite) need to be buried quickly to minimize oxidation by bacterial processes acting to decay organic material, which is also washed in during storm events (Hilton et al. 1986). Spikes in CHI, therefore, represent a sedimentological response to storm events and are typically associated with spikes in sand, capped by elevated %TOM (i.e., organic material settling out after being washed in). In some core sections CHI is very low, despite the presence of high sand content. And, as previously stated, high sand content is interpreted to represent increased wetness or storminess. The combination of low CHI and high sand also occurs in the presence of elevated %TOM (another indication of increased wetness). Therefore, in cases where low CHI is associated with high sand and high %TOM, we interpret the low CHI as reflecting a the diagenesis of the magnetic sediment fraction due to the bacterial oxidation of associated organic material. Together, the occurrence of elevated %sand with high or low CHI, %TOM, and charcoal constitute rapidly deposited layers. These features are interpreted as indicators of discrete storm events.

Early Holocene climate (9000–7500 cal year B.P.)

Given the alpine setting of Dry Lake (2763 m), it is likely that ice covering the lake in winter months

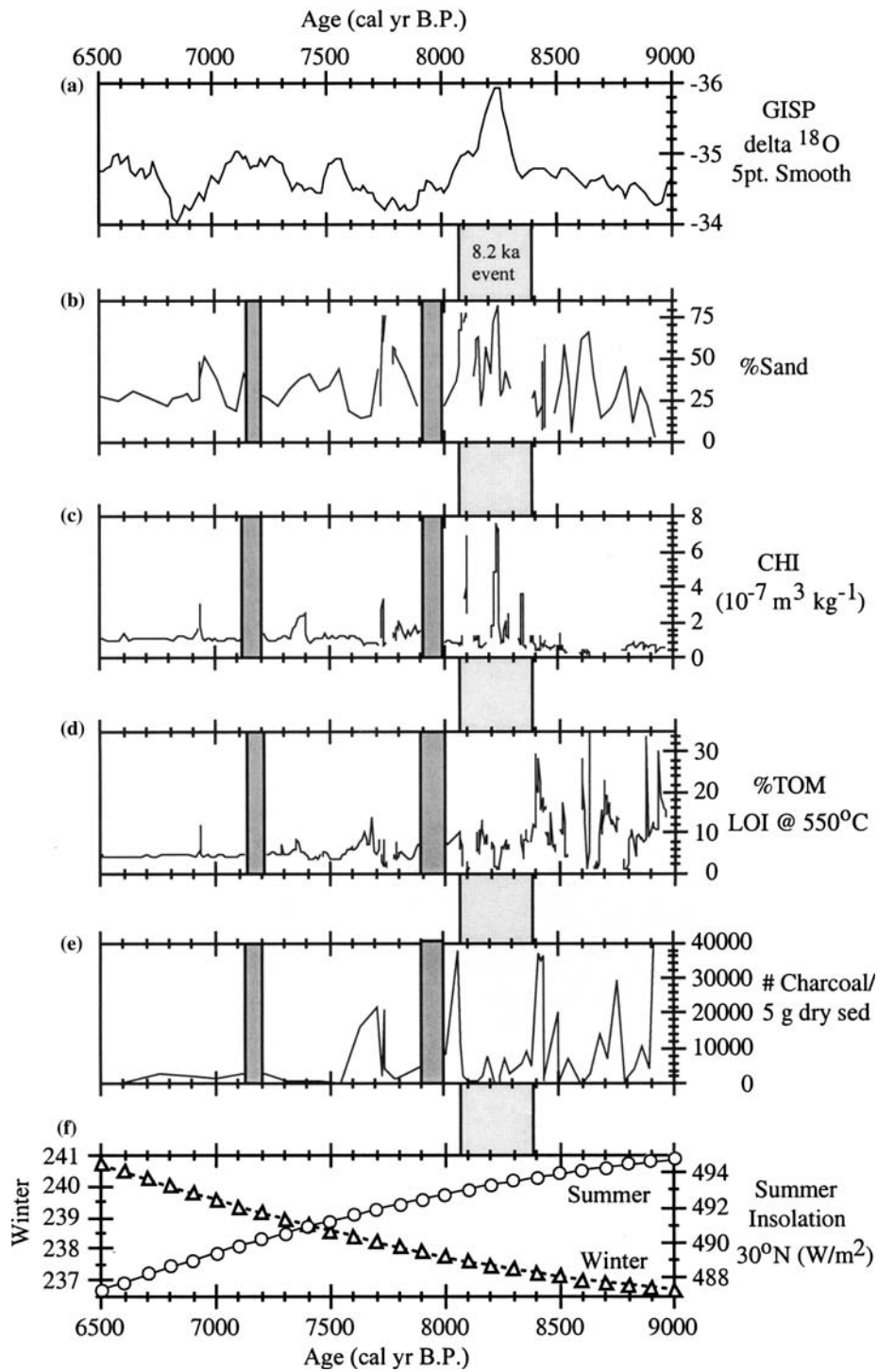


Figure 4. Comparison of (a) reversed axis GISP $\delta^{18}\text{O}$ 5 pt. smoothed data (Alley et al. 1993) with (b) %sand; (c) mass magnetic susceptibility; (d) %TOM and (e) number of charcoal grains per 5 g dry sediment from DL as well as with (f) summer insolation for 30° N latitude. The box denotes the 8.2 ka event 'interval' as identified in Dry Lake.

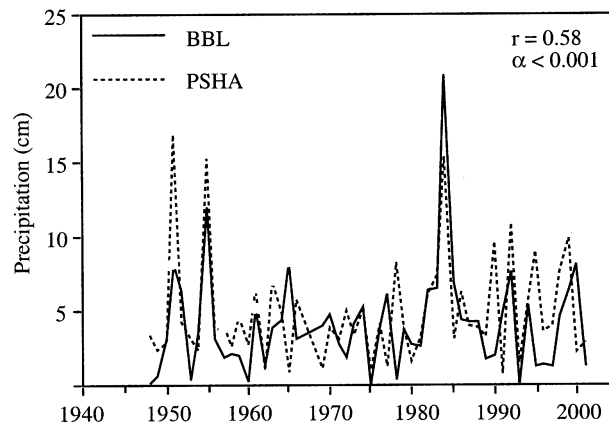


Figure 5. Comparison of July–August precipitation data from Phoenix Sky Harbor Airport, AZ (PSHA) and Big Bear Lake, CA (BBL). Note the exceptionally strong monsoon seasons of 1951, 1955, and 1984 (precipitation > 1SD) are synchronous between BBL and PSHA, demonstrating that modern summer precipitation in the San Bernardino Mountains is influenced by the NAM.

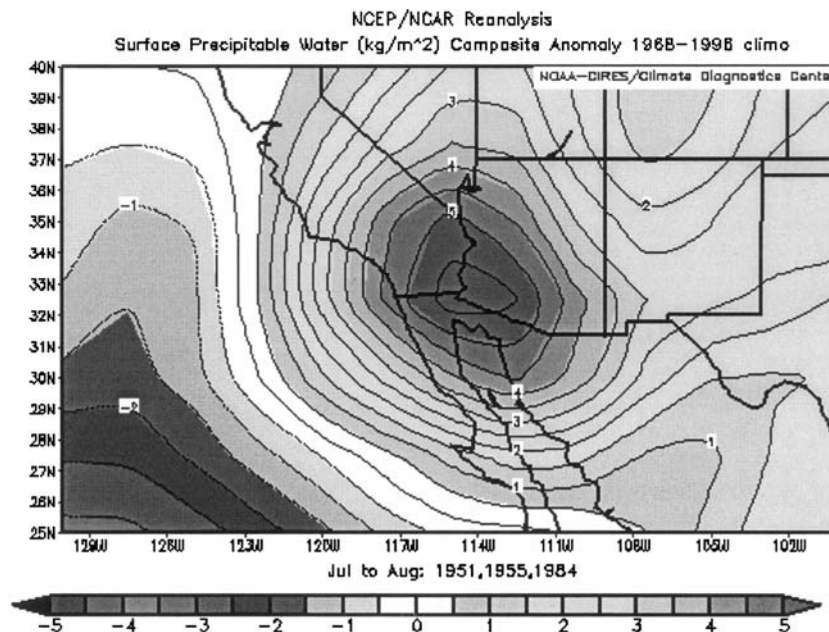


Figure 6. Plot of anomalous July–August precipitable water during the severe monsoon seasons of 1951, 1955, and 1984, created using the NCEP/NCAR interactive reanalysis database (<http://www.cdc.noaa.gov/cgi-bin/Composites/printpage.pl>). Note the large positive anomaly is centered over southern California and Arizona, illustrating the regional expansion of the NAM into the San Bernardino Mountains during these years.

shielded the basin from the deposition of RDLs during the winter season (e.g., Ohlendorf et al. 2000). In addition, precipitation at Dry Lake during the modern winter season is received primarily as snow (Minnich 1984). Therefore, during the early Holocene, when winter insolation was at a minimum, resulting in cooler winters in southern

California (Kirby et al. 2005), it is likely that precipitation was also overwhelmingly received as snow. Furthermore, spring snowmelt is not rapid enough to produce the energy required to transport the observed thick sand layers to the lake's depocenter. Therefore, we suggest that the source of the early Holocene RDLs, and therefore general

storminess, at Dry Lake are variations in summer precipitation.

As the analysis of historical precipitation data demonstrates, summer precipitation during the NAM season at Big Bear (and thus Dry Lake) is significantly correlated with monsoonal precipitation at Phoenix. Figure 5 shows that the exceptionally strong monsoon seasons of 1951, 1955, and 1984 (precipitation $>1SD$) were regionally extensive, resulting in contemporaneous extreme precipitation at Big Bear and Phoenix. As well, anomalous precipitable water plots for these years, demonstrates that the regional extent of the NAM was expanded to include both Arizona and southern California (Figure 6). Additionally, Tubbs (1972) documented that strong NAM seasons effect the Transverse and Peninsular Ranges of southern California. Therefore, because the NAM is strongly linked to increased summer insolation, and early Holocene insolation was significantly stronger, we ascribe the wet early Holocene climate at Dry Lake to an insolationally enhanced NAM. This conclusion is supported by the climate modeling studies of Webber (2001) and Liu et al. (2003), who modeled a strengthened early Holocene NAM in response to elevated summer insolation.

Using the well-defined relationships between summer insolation and the modern NAM, we can infer how increased summer insolation during the early Holocene may have influenced the NAM. With higher summer insolation during the early Holocene, SSTs would have warmed in the GOC to the 26°C threshold temperature more rapidly, initiating early monsoonal precipitation and sustaining it longer into the fall season. Furthermore, increased early Holocene summer insolation may have caused GOC SSTs to surpassed the second threshold temperature of 29°C more frequently, creating more regular extreme monsoon events. Elevated early Holocene summer insolation would have also enhanced SSTs in the eastern tropical Pacific, thereby deepening convection in the region and significantly bolstering atmospheric moisture available to the NAM, particularly for coastal regions. These inferences are supported by studies from the Santa Barbara Basin (SBB) by Pisias (1978) and Friddell et al. (2003), which indicate that the eastern tropical Pacific was warmer than present during the early Holocene. As well, pollen studies from the SBB indicate that the southwest

was generally wetter during the early Holocene (Heusser 1978). Enhanced SSTs in the eastern tropical Pacific during the early Holocene, driven by greater summer insolation, is likely to have generated stronger and more frequent easterly tropical waves and associated disturbances (i.e., cyclones), thereby enhancing moisture surges and strengthening the NAM. The early Holocene summer insolation maximum would also have strengthened regional anticyclonic atmospheric circulation. Strengthened anticyclonic circulation would in turn advect more warm moist air from the eastern tropical Pacific and GOC into the southwest, supplying greater moisture to the monsoon region. Furthermore, vigorous vertical atmospheric movement associated with the strong thermal low would generate convective storm activity associated with the NAM, particularly in concert with the orographic effect of the San Bernardino Mountains.

The Dry Lake record supports these inferences and indicates the coastal southwest was wetter and stormier between 9000 and 7500 than at present, which we ascribe to an enhanced NAM (Figure 4). Generally high sand percentages and frequent sand spikes capped by organic rich units indicate a sustained energetic depositional environment punctuated by frequent RDLs. Generally elevated %TOM and charcoal, in addition to the presence of organic rich layers, which consist almost exclusively of charcoal and wood fragments, suggest high basin productivity and significant fluvial transport of terrestrially derived organic material into Dry Lake during storm events associated with the NAM (Figure 4). Low CHI values from 9000 to 8400 further supports a wet, productive environment at Dry Lake, as the overwhelming input of organic material, and subsequent bacterial decay, oxidized the magnetic fraction, resulting in anomalously low CHI during this interval (Figure 4). After 7500, summer precipitation at Dry Lake appears to have diminished, as indicated by decreased variability in all proxies (Figure 4).

The interpretation of the Dry Lake record is supported by both regional paleoclimate and recent climate modeling studies. Davis and Shafer (1992) recognized an early Holocene 'moist interval' at Montezuma Well, AZ, that was associated with an increase in pollen from plant species adapted to utilize summer precipitation, suggesting increased monsoonal precipitation. Other

studies, such as Enzel et al. (1992) and more recently, Kirby et al. (2005), also indicate that the early Holocene was wetter than the modern climate, although the resolution and location of these records precludes their ability to draw specific conclusions concerning relative seasonal contributions. Additionally, the results of modeling studies by Webber (2001) and Liu et al. (2003) suggest that increased early Holocene summer insolation served to strengthen NAM in the southwestern United States.

In summary, elevated insolation during the early Holocene enhanced the NAM by increasing summer SSTs in the GOC and eastern tropical Pacific. Elevated SSTs generated more frequent easterly tropical waves, which in turn created more moisture surges, in addition to strengthening regional atmospheric circulation. We propose the anomalously far-reaching monsoon seasons of the 20th century are analogs for the 'normal' NAM activity during the early Holocene. The net result was a wetter, stormier early Holocene summer climate in the coastal southwest. This interpretation is supported by sedimentological evidence from Dry Lake, which indicates increased summer storminess and precipitation during the early Holocene. The interpretation is further supported by regional paleoclimate studies and model studies, which suggest the early Holocene was wetter in response to a stronger NAM.

The 8.2 ka event?

Superimposed on the early Holocene NAM signal is a 300-year interval from 8400 to 8100, apparently without significant monsoonal activity in the San Bernardino Mountains (Figure 4). We attribute this cold snap to the 8.2 ka event recognized in the GISP ice core (Alley et al. 1997). Since the initial discovery of the 8.2 ka event in the GISP ice core, mounting global evidence from terrestrial, marine, and ice records from Mexico, the Netherlands, Eastern Europe, Costa Rica, and Tibet, suggest that the event was a significant widespread cool climate anomaly (Ninglian et al. 2002; Lanchriet et al. 2004; Seppä and Poska 2004; Vázquez-Selem and Heine 2004; Wagner et al. 2004). In addition, studies suggest that what is referred to as the 8.2 ka event is in fact a longer-term cold climate anomaly with an additional

abrupt cold climate anomaly super imposed on the greater long-term event structure (Rohling and Pälike 2005).

While the aforementioned studies compellingly demonstrate the global nature of the 8.2 ka event, the southwestern United States response to the event has remained elusive. For example, Clark et al. (2003) found no evidence of an 8.2 ka event related glacial advance from alpine lakes in the Sierra Nevada. As well, published marine records from the Santa Barbara Basin show no significant cooling during the early Holocene (Friddell et al. 2003). New $\delta^{18}\text{O}$ data from *G. bulloides* and *N. pachyderma* from the Santa Barbara Basin, however, appear to indicate a distinct cool period with shallowing of the thermocline and weakening stratification of the upper water column associated with the 8.2 ka event (Kennett 2005). Furthermore, Davis and Shafer (1992) identified a dramatic cold interval between 7780 and 7940 at Montezuma Well, previously unassociated with the 8.2 ka event. During this event, summer precipitation decreased and temperatures drop to their lowest values for the site (approximately 4 °C decrease), and winter precipitation increased (Davis and Shafer 1992). Significant to the Dry Lake record, Owen et al. (2003) identified, through cosmogenic dating, an early Holocene glacial advance in the San Bernardino Mountains some time between 9000 and 5000. Given that previous advances were associated with perturbations in North Atlantic thermohaline circulation (e.g., Heinrich Event 1 and the Younger Dryas), it is plausible that the early Holocene advance is associated with the 8.2 ka event, which itself is linked to a perturbation in the North Atlantic thermohaline circulation (Barber et al. 1999). The Dry Lake record, with its well-dated sediment record and its proximity to the glacial features dated by Owen et al. (2003), is a suitable location to explore how the coastal southwest responded to the 8.2 ka event and if the resulting climate could support the growth and maintenance of glacier in the San Bernardino Mountains.

The 8.2 ka event at Dry Lake is characterized by depressed charcoal and %TOM, and elevated CHI and %sand from 8400 to 8100, which occur contemporaneously with the negative $\delta^{18}\text{O}$ anomaly recognized as the 8.2 ka event in the GISP ice core (Alley et al. 1997; Figure 4a–e). These relationships suggest that basin biomass decreased in

response to colder summer temperatures and suppressed monsoonal precipitation, which in turn increased local erosion. Cooler summer temperatures in combination with a sustained, southerly winter jet stream would have led to significant snow accumulation in the San Bernardino Mountains and potentially glacier formation. These conclusions are consistent with the findings of Davis and Shafer (1992), who found monsoonal precipitation during the 8.2 ka event was significantly reduced. Davis and Shafer (1992) also noted total precipitation appeared greater, which suggests winter precipitation increased in response to a more sustained, southerly winter jet stream. Notably, other proxy records of early Holocene monsoon activity from Africa and Costa Rica also demonstrate a reduction in monsoonal precipitation that is contemporaneous with the reduction noted at Dry Lake (Gasse 2000; Lachniet et al. 2004).

The climatic conditions at Dry Lake appear to support a glacial response to the 8.2 ka event in the San Bernardino Mountains. Cooler summers in concert with enhanced winter precipitation for a sustained 300-year period would allow for perennial snow to persist in the San Bernardino Mountains, particularly on the shaded northern slopes of San Gorgonio. Therefore, it is our conclusion that the 8.2 ka event is the best candidate for the early Holocene glacial advance identified by Owen et al. (2003).

Conclusions

Recent synoptic and modeling studies of the NAM and newly developed climate records from Dry Lake provide new insight into the complex relationships between early Holocene insolation and climate in the coastal southwest. Proxy data from Dry Lake indicate a wet, stormy early Holocene from 9000 to 7500 followed by decreasing storminess to 6500. This wet period is attributed to an enhanced NAM, strengthened by the early Holocene summer insolation maximum.

Superimposed on the early Holocene NAM signal is the 8.2 ka event. This globally documented climate perturbation, previously unrecognized in the coastal southwest, registers at Dry Lake as a 300-year cold period characterized by decreased summer monsoonal precipitation,

decreased basin productivity, and enhanced local erosion. Owen et al. (2003) identified an early to middle Holocene (9000–5000) glacial moraine near Dry Lake in the San Bernardino Mountains. Based on sedimentological evidence from Dry Lake, we conclude the 8.2 ka event is the most likely interval for the proposed glacial advance.

Acknowledgements

We would like to thank the Petroleum Research Fund (grant: ACS/PRF 41789-GB8) and the National Science Foundation (grant: EAR-IF: #0318511) for helping to make this research possible. Special thanks to Gabe Filippelli, Kathy Licht, and Andrew Barth for their participation in coring Dry Lake. We would also like to acknowledge Dr. John Southon and Dr. Guaciara dos Santos for their assistance and input on age control for the cores. As well, we thank the rangers at the Mill Creek Ranger station for their assistance in accessing the Dry Lake, with special recognition to Val Silve for providing mule transportation. Finally, we thank Dr. William Last and an anonymous reviewer for their comments, which served to improve this manuscript.

References

- Adams D.K. and Comrie A.C. 1997. The North American monsoon. *B. Am. Meteorol. Soc.* 78: 2197–2213.
- Alley R.B., Messe D.A., Shuman C.A., Gow A.J., Taylor K.C., Grootes P.M., White J.W.C., Ram M., Waddington E.D., Mayewski P.A. and Zielinski G.A. 1993. Abrupt increase in Greenland snow accumulation at the end of the Younger Dryas event. *Nature* 362: 527–529.
- Alley R.B., Mayewski P.A., Sowers T., Stuiver M., Taylor K.C. and Clark P.U. 1997. Holocene climate instability: a prominent, widespread event 8200 yr ago. *Geology* 25: 483–486.
- Barber D.C., Dyke A., Hillaire-Marcel C., Jennings A.E., Andrews J.T., Kerwin M.W., Bilodeau G., McNeely R., Southon J., Morehead M.D. and Gagnon J.M. 1999. Forcing of the cold event of 8200 years ago by catastrophic drainage of Laurentide Lakes. *Nature* 400: 344–348.
- Brenner I.S. 1974. A surge of maritime tropical air-Gulf of California to the southwestern United States. *Mon. Weather Rev.* 102: 375–389.
- Boyle J. 2004. A comparison of two methods for estimating the organic matter content of sediments. *J. Paleolimnol.* 31: 125–127.
- Cayan D.R. and Roads J.O. 1984. Local relationships between United States west coast precipitation and monthly mean circulation parameters. *Mon. Weather Rev.* 112: 1276–1282.

- Cayan D.R., Roads J.O., Redmond K.T. and Riddle L.G. 1999. ENSO and Hydrologic extremes in the western United States. *J. Climate* 12: 2881–2893.
- Clark D., Gillespie A.R., Clark M. and Burke B. 2003. Mountain glaciations of the Sierra Nevada. In: Easterbrook D.J. (ed.), *Quaternary Geology of the United States. INQUA 2003 Field Trip Guide Volume*, Desert Research Institute, Reno, NV, pp. 287–311.
- Clark D., Gillespie A.R., Clark M., Burke B. and Shafer D.S. 1992. A Holocene climatic record for the Sonoran Desert from pollen analysis of Montezuma Well, Arizona, USA. *Palaeogeogr. Palaeoclimatol.* 92: 107–119.
- Dean W.E. 1974. Determination of carbonate and organic matter in calcareous sedimentary rocks by loss on ignition: Comparison with other methods. *J. Sediment. Petrol.* 44: 242–248.
- Ely L.L., Enzel Y. and Cayan D.R. 1994. Anomalous North Pacific atmospheric circulation and large winter floods in the southwestern United States. *J. Climate* 7: 977–987.
- Enzel Y., Brown W.J., Anderson R.Y., McFadden L.D. and Wells S.G. 1992. Short-duration Holocene Lakes in the Mojave River Drainage Basin, southern California. *Quaternary Res.* 38: 60–73.
- Fridell J.E., Thunell R.C., Guilderson T.P. and Kashgarian K. 2003. Increased northeast Pacific climate variability during the warm middle Holocene. *Geophys. Res. Lett.* 30: 14-1–14-4.
- Gasse F. 2000. Hydrological changes in the African tropics since the last glacial maximum. *Quat. Sci. Rev.* 19: 189–211.
- Hales J.E.Jr. 1972. Surges of maritime tropical air northward over the Gulf of California. *Mon. Weather Rev.* 100: 298–306.
- Heiri O., Andre F.L. and Lemcke G. 2001. Loss on ignition as a method for estimating organic and carbonate content in sediments: reproducibility and comparability of results. *J. Paleolimnol.* 25: 101–110.
- Hereford R., Webb R.H. and Longpre C.I. 2004. *Precipitation History of the Mojave Desert Region, 1893–2001*. USGS Fact Sheet 117–03 3 pp.
- Heusser L. 1978. Pollen in the Santa Barbara Basin, California, A 12,000-yr record. *Geol. Soc. Am. Bull.* 89: 673–678.
- Higgins R.W., Shi W. and Hain C. 2004. Relationships between Gulf of California moisture surges and precipitation in the southwestern United States. *J. Climate* 17: 2983–2997.
- Hilton J., Long G. J., Chapman J.S. and Lishman J.P. 1986. Iron mineralogy in sediments: a Mossbauer Study, *Geochim. Cosmochim. Acta* 50: 2147–2151.
- Hirschboeck K.K. 1985. *Hydroclimatology of flow events in the Gila River Basin, central and southern Arizona*: Tucson. PhD. diss. University of Arizona, 355 pp.
- Kalnay E., Kanamitsu M., Kistler R., Collins W., Deaven D., Gandin L., Iredell M., Saha S., White G., Woolen J., Zhu Y., Chelliah M., Ebisuzaki W., Higgins W., Janowiak J., Mo K.C., Ropelewski C., Wang J., Leetmaa A., Reynolds R., Jenne R. and Joseph D. 1995. The NCEP/NCAR 40 year Reanalysis Project. *B. Am. Meteorol. Soc.* 77: 437–471.
- Kennett D.J. 2005. *The Island Chumash: Behavioral Ecology of a Maritime Society*, University of California Press, London, pp. 41–71.
- Kirby M.E., Lund S.P. and Poulsen C.J. 2005. Hydrologic variability and the onset of modern El Niño-Southern Oscillation: a 19,250-year record from Lake Elsinore, southern California. *J. Quaternary Sci.* 20: 239–254.
- Lanchiet M.S., Asmerom Y., Burns S.J., Patterson W.P., Polyak V.J. and Seltzer G.O. 2004. Tropical response to the 8200 yr B.P. cold event?: Speleothem isotopes indicate a weakened early Holocene monsoon in Costa Rica *Geology* 32: 957–960.
- Lanci L., Hirt A.M., Lowrie W., Lotter A.F., Lemcke G. and Sturm M. 1999. Mineral-magnetic record of Lake Quaternary climatic changes in a high Alpine lake. *Earth Planet. Sci. Lett.* 70: 49–59.
- Liu Z., Otto-Bliesner B., Kutzbach J., Li L. and Shields C. 2003. Coupled climate simulation of the evolution of global monsoons in the Holocene. *J. Climate* 16: 2472–2490.
- MacDonald G.M., Larsen C.P.S., Szeicz J.M. and Moser K.A. 1991. The reconstruction of Boreal forest fire history from lake sediments: a comparison of charcoal, pollen, sedimentological, and geochemical indices. *Quaternary Sci. Rev.* 10: 53–71.
- Mitchell D.L., Ivanova D., Rabin R., Brown T.J. and Redmond K. 2002. Gulf of California sea surface temperatures and the North American monsoon: Mechanistic implications from observations. *J. Climate* 15: 2261–2281.
- Minnich R.A. 1984. Snow drifting and timberline dynamics on Mount San Geronio, California, U.S.A.. *Arctic Alpine Res.* 16: 395–412.
- Minnich R.A. 1986. Snow levels and amounts in the mountains of southern California. *J. Hydrol.* 89: 37–58.
- Mo K.C. and Higgins W.R. 1998. Tropical influences on California Precipitation. *J. Climate* 11: 412–430.
- Morton D.M., Cox B.F. and Matti J.C. 1980. *Geologic Map of the San Geronio Wilderness, San Bernardino Wilderness, San Bernardino County, California [map]*. 1:62500. USGS, Washington D.C.
- Ninglian W., Tandong Y., Thompson L.G., Henderson K.A. and Davis M.E. 2002. Evidence for cold events in the early Holocene from the Guliya ice core, Tibetan Plateau, China. *Chinese Sci. Bull.* 47: 1422–1427.
- Ohlendorf C., Bigler C., Goudsmit G., Lemcke G., Livingstone G.M., Lotter A.F., Muller B. and Sturm M. 2000. Causes and effects of long periods of ice cover on a remote high Alpine lake. *J. Limnol.* 59: 65–80.
- Owen L.A., Finkel R.C., Minnich R.A. and Perez A.E. 2003. Extreme Southwestern Margin of Late Quaternary Glaciation in North America: timing and controls. *Geology* 31: 729–732.
- Pisias N.G. 1978. *Paleoceanography of the Santa Barbara Basin during the last 8000 years*. *Quaternary Res.* 10: 366–384.
- Pyke C.B. 1972. *Some meteorological aspects of the seasonal distribution of precipitation in the western United States and Baja California*. University of California Water Resources Center Contribution, no. 139, 205 pp.
- Redmond K.T. and Kotch R.W. 1991. Surface climate and streamflow variability in the western United States and their relationship to large-scale circulation indices. *Water Resour. Res.* 27: 2381–2399.
- Rohling E.J. and Pälike H. 2005. Centennial-scale climate cooling with a sudden cold event around 8200 years ago. *Nature* 434: 975–979.

- Ropelewski C.F. and Halpert M.S. 1986. North American precipitation and temperature patterns associated with El Niño-Southern Oscillation (ENSO). *Mon. Weather Rev.* 114: 2352–2362.
- Schonher T. and Nicholson S.E. 1989. The Relationship between California Rainfall and ENSO Events. *J. Climate* 2: 1258–1269.
- Seppä H. and Posky A. 2004. Holocene annual mean temperature changes in Estonia and their relationship to solar insolation and atmospheric circulation patterns. *Quaternary Res.* 61: 22–31.
- St-Onge G., Mulder T., Piper D.J.W. Hillaire-Marcel C. and Stoner J. 2004. Earthquake and flood induced turbidities in the Saguenay Fjord (Québec): a Holocene paleoseismicity record. *Quaternary Sci. Rev.* 23: 283–294.
- Stuiver M. and Polach H.A. 1977. Discussion; reporting of C-14 data. *Radiocarbon* 19: 355–363.
- Stuiver M., Polach H.A. and Reimer P.J. 1993. Extended ¹⁴C database and revised CALIB radiocarbon calibration program. *Radiocarbon* 35: 215–230.
- Thompson R., Battarbee R.W., O'Sullivan P.E. and Oldfield F. 1975. Magnetic susceptibility of lake sediments. *Limnol. Oceanogr.* 20: 687–698.
- Trewartha G.T. 1981. *The Earth's Problem Climates*. University of Wisconsin Press, Madison, pp. 297–310.
- Tubbs A. 1972. Summer thunderstorms over southern California. *Mon. Weather Rev.* 100: 701–710.
- U.S. Geological Survey 1996. Moonridge Quadrangle, California [map]. 1:24,000. 7.5 Minute Series. USGS, Washington DC.
- U.S. Geological Survey 1996. San Gorgonio Quadrangle, California [map]. 1:24,000. 7.5 Minute Series. USGS, Washington DC.
- Vázquez-Selem L. and Heine K. 2004. Late Quaternary glaciations of México. In: Ehlers J. and Gibbard P.L. (eds), *Quaternary Glaciations-Extent and Chronology. Part III*, pp. 233–242.
- Wagner F., Kouwenberg L.L.R., van Hof T.B. and Visscher H. 2004. Reproducibility of Holocene atmospheric CO₂ records based on stomatal frequency. *Quaternary Sci. Rev.* 23: 1947–1954.
- Warner N.R. and Domack E.W. 2002. Millennial- to decadal-scale paleoenvironmental change during the Holocene in the Palmer Deep, Antarctica, as recorded by particle size analysis. *Paleoceanography* 17: 5-1–5-14.
- Weaver R. 1962. *Meteorology of hydrologically critical storms in California*. Hydrometeorological Report No. 37, U.S. Weather Bureau, 207 pp.
- Webb R.H. and Betancourt J.L. 1992. Climatic variability and flood frequency of the Santa Cruz River, Pima County, Arizona. U.S. Geological Survey Water-Supply Paper 2379.
- Webber S.L. 2001. The impact of orbital forcing on the climate of an intermediate-complexity coupled model. *Global and Planet. Change* 30: 7–12.